DTU Wind Energy Report

# Perdigão 2017: DTU's scanning lidar measurements

Robert Menke, Nikola Vasiljevic, Jakob Mann

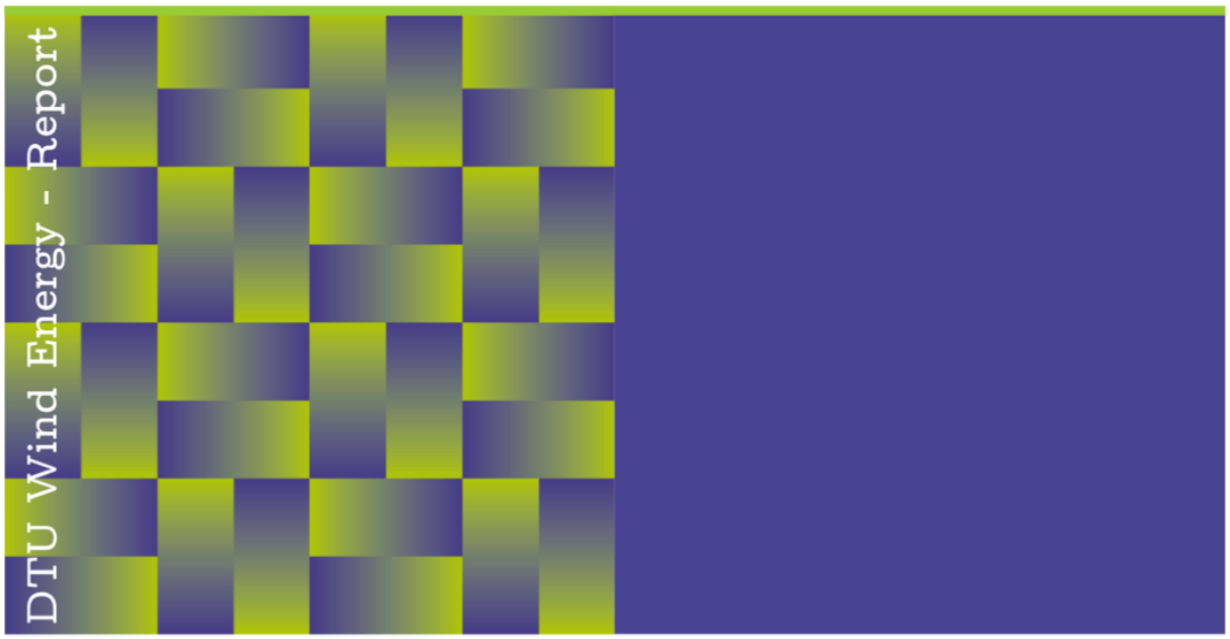


NEW EUROPEAN WIND ATLAS
newa

DTU Wind Energy
Department of Wind Energy

**Author:** Robert Menke, Nikola Vasiljevic, Jakob Mann
**Title:** Perdigão 2017: DTU's scanning lidar measurements
**Department:** DTU Wind Energy

**DTU Wind Energy Report**
**July 26, 2019**

**Version: 1.0**

**Abstract:**
This report contains information about scanning trajectories and measurement data availability of the scanning lidar schemes performed by DTU during the field experiment Perdigão 2017 in Portugal.

Data DOI: https://doi.org/10.11583/DTU.7228544.v1

Version 1.0 - 01 June 2019 - Initial Document Release

**Sponsorship:**
**NEWA**

**Pages:** 10
**Tables:** 3
**Figures:** 4
**References:** 8

Contacts:
Robert Menke
rmen@dtu.dk
Jakob Mann
jmsq@dtu.dk
Nikola Vasiljevic
niva@dtu.dk

Technical University of Denmark
Frederiksborgvej 399
4000 Roskilde
Denmark

# Contents

# 1 Introduction

This report contains information about scanning trajectories and measurement data availability of the scanning lidar schemes performed by DTU during the field experiment Perdigão 2017 in Portugal. A general overview about the measurement campaign has been published by Fernando et al (2019). Details about the all lidar scans performed during the campaign can be found in planning report (Vasiljevic et al, 2017).

# 2 WindScanner locations

The 8 WindScanners operated by DTU were positioned on the ridge crests, four on each ridge. The position of the WindScanner is shown in figure 1 and table 1 contains the exact locations. This information is an excerpt from the official report containing the coordinates of all instruments that were deployed during the campaign (Palma et al, 2018).

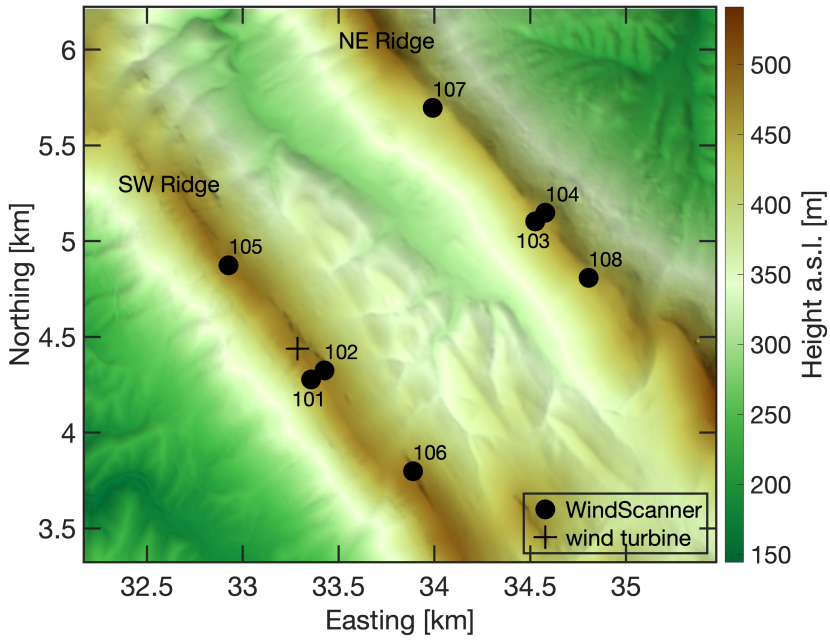


*Figure 1. Position of WindScanners.*

*Table 1. Positions of WindScanners. Easting and northing in PT-TM06 / ETRS89 coordinate system and elevation above sea level. Elevation of the WindScanners refers to the scanner head position.*

| Station Number | Station Acronym | Easting [m] | Northing [m] | Elevation [m] |
|---|---|---|---|---|
| 101 | LRWS #1(DTU) | 33356.3 | 4277.6 | 470.4 |
| 102 | LRWS #2(DTU) | 33426.2 | 4324.1 | 480.3 |
| 103 | LRWS #3(DTU) | 34526.4 | 5103.5 | 452.3 |
| 104 | LRWS #4(DTU) | 34578.9 | 5147.7 | 454.9 |
| 105 | LRWS #5(DTU) | 32926.5 | 4874.3 | 485.9 |
| 106 | LRWS #6(DTU) | 33888.7 | 3798.0 | 486.3 |
| 107 | LRWS #7(DTU) | 33990.6 | 5695.3 | 437.1 |
| 108 | LRWS #8(DTU) | 34804.6 | 4807.9 | 452.8 |

# 3 Scanning schemes

The scanning scheme did not change compared to our initial suggestion during the design process of the scanning trajectories (Vasiljevic et al, 2017). Four of the scanners performed continuously RHI scans along a transect perpendicular to the ridges and the four remaining ones alternated between three different measurement scenarios. Each scenario was measured for 10 minutes. The different intervals are illustrated in table 2 and the different scanning scenarios are briefly explained in the following sections.

*Table 2. Scanning intervals. Interval 1 was executed in the 10 min periods from hh:10 - hh:20 and hh:40 - hh:50, Interval 2 from hh:20 - hh:30 and hh:50 - hh:00, and Interval 3 from hh:00 - hh:10 and hh:30 - hh:40*

| 10min Interval / WindScanner | 1 | 2 | 3 |
|---|---|---|---|
| **LRWS #1** | Transect Scan - transect 2 | | |
| **LRWS #2** | | | |
| **LRWS #3** | | | |
| **LRWS #4** | | | |
| **LRWS #5** | Ridge Scan (NE ridge) | VM Scan (VM1) | Transect Scan (transect 1) |
| **LRWS #6** | | VM Scan (VM2) | Transect Scan (transect 3) |
| **LRWS #7** | Ridge Scan (SW ridge) | VM Scan (VM3) | RHI Scan (transect 1) |
| **LRWS #8** | | VM Scan (VM4) | Transect Scan (transect 3) |

## 3.1 Transect scans

The three transect scans are consisting of 2-4 RHI scans that are executed in the same vertical plane. All transects are nearly perpendicular to the two ridges (see figure 3). We measured continuously during the upwards movement of the scanners with an averaging elevation angle of 0.75° over a range of 36°. Range gates were placed every 15 m, starting at a range of 100 m, extending to 3000 m. Details about orientation of the transects and data availability can be found in the following publication Menke et al (2019). To emphasize again: measurements along transects 2 were carried out continuously whereas the RHI scans along transect 1 and 3 were carried out for two 10-minute intervals per hour (see table 2). An animation of the measurements along transect 2 for the period of the Intensive Operation Period (IOP) is available under the following link: https://youtu.be/I5luRZ7NXZA.

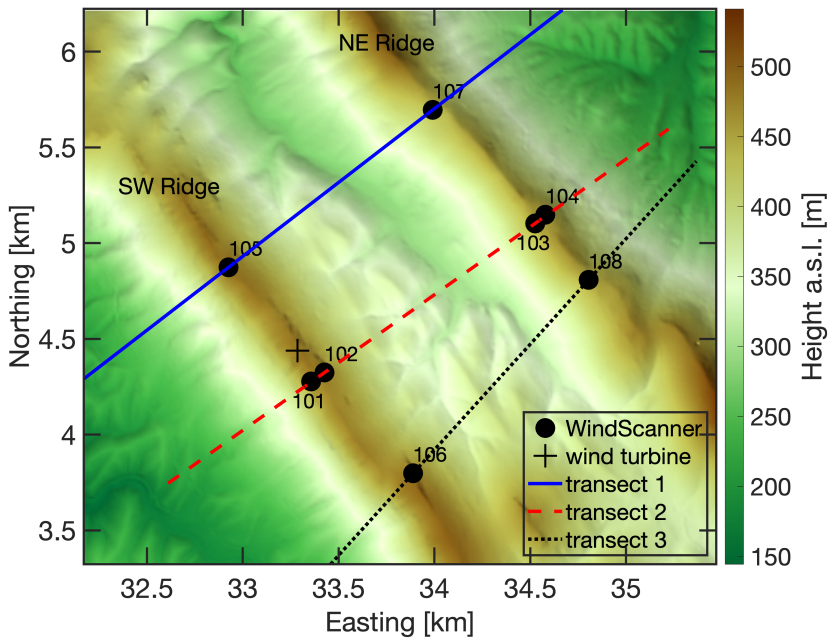


*Figure 2. Orientation of the three transects scans and location of WindScanners.*

## 3.2 Ridge scans

For the ridge scans, pairs of lidars followed the height profile of the ridges in horizontal direction in 80 m height. WindScanner 107 and 108 measured above the SW ridge and 105 and 106 above the NE ridge. In total 92 measurement points along a 1.8 km long transects were measured. The measurements of the two lidars along the same complex trajectory can be combined to retrieve wind vectors in a nearly horizontal plane. Additionally, range gates are placed every 10 m before and after the ridge positions, starting at 700 m, and extending to 2640 m. Data of these scans was used in the following publications: Barthelmie et al (2018); Mann et al (2018).

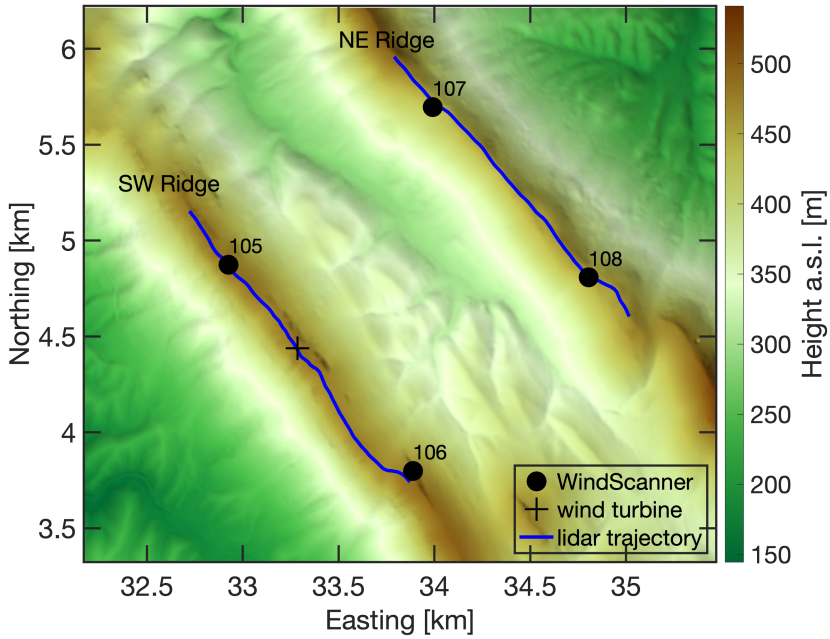


*Figure 3. Ridge scan trajectories.*

## 3.3 Virtual mast scans

Four virtual masts were created by crossing two RHI scans at the four locations shown in figure 4 and exact coordinates in table 3. The virtual masts are starting about 80 m above ground level and VM1, VM2 and VM3 are collocated with the 100 m measurement masts. For VM1 the RHI scans of 103 and 105 have to be combined, for VM2 the RHI scans of 102 or 103 with 106, for VM3 the RHI scans of 102 and 107, and for VM3 the RHI scans of 104 and 108. The RHI scans of 105-8 have the same characteristics as described in section 3.1 despite that 105 and 107 only cover a range of 18° instead of 36°.

*Table 3. Coordinates of virtual mast locations.*

| Name | Easting [m] | Northing [m] |
|---|---|---|
| VM1 | 33372.7 | 4286.2 |
| VM2 | 34151.0 | 4837.6 |
| VM3 | 34536.4 | 5110.6 |
| VM4 | 34771.3 | 5284.0 |

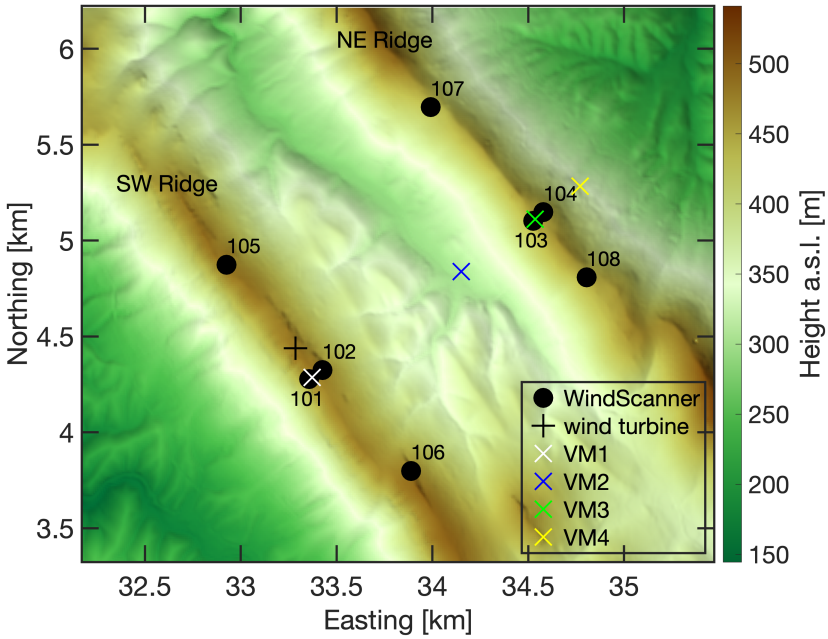


*Figure 4. Virtual mast locations.*

# 4 Data Structure and Access

The data has been converted to the *nedcdf* format following the conventions as outlined in Vasiljevic et al (2019) and the files are sorted by scenario and are available via the DTU/NCAR data archives: (Menke et al, 2018). The data is also available on the mirrored Perdigão data archives in the folder *data/DTU_WindScanner/netcdf*.

# Bibliography


Palma, J. M. L. M., Menke, R., Mann, J., Oncley, S., Matos, J. and Lopes A.S.: Perdigão–2017: experiment layout, https://perdigao.fe.up.pt/ → Documents → Reports → Perdigao Experiment Layout Version 1.pdf, 2018.

Vasiljevic, N., Mann, J., Menke, R. et al: Perdigão 2017 Science Plan: Scanning lidar, https://perdigao.fe.up.pt/ → Documents → Reports → 20170228.Perdigao_Scanning_Lidar_Layout_Final.pdf, 2017.

Menke, R., Vasiljević, N., Mann, J. and Lundquist, J.K.: Characterization of flow recirculation zones at the Perdigão site using multi-lidar measurements, Atmos. Chem. Phys., 19, 2713-2723, https://doi.org/10.5194/acp-19-2713-2019, 2019.

Barthelmie, R.J. et al 2018 J. Phys.: Conf. Ser. 1037 052022, https://doi.org/10.1088/1742-6596/1037/5/052022, 2018.

Mann, J. et al 2018 J. Phys.: Conf. Ser. 1037 072017, https://doi.org/10.1088/1742-6596/1037/7/072017, 2018.

Vasiljevic, N., Klaasen, T. et al: e-WindLidar: making wind lidar data FAIR, http://e-windlidar.windenergy.dtu.dk/document/report.pdf, 2019.

Menke, R., Vasiljevic, N., Mann, J.: Perdigão-2017: multi-lidar flow mapping over the complex terrain site, https://doi.org/10.11583/DTU.7228544.v1, 2018.

Fernando, H. J. S., et al: The Perdigão: Peering into Microscale Details of Mountain Winds, Bulletin of the American Meteorological Society 2018, https://doi.org/10.1175/BAMS-D-17-0227.1, 2019.